Dust Formation in AGB Stars

The Case of Silicon Carbide

Dave Nero

Fall 2009

Outline

AGB Stars

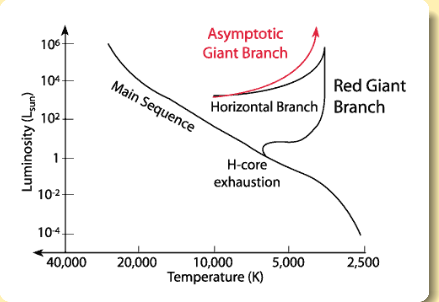

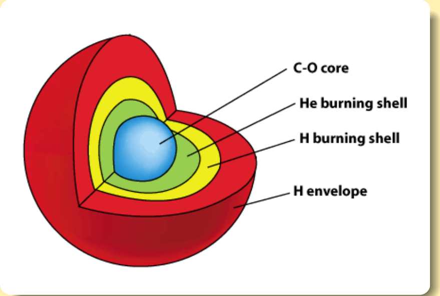

Origin and Characteristics

- Stellar evolution
- Nucleosynthesis

Images from NOAO

Dust Factories

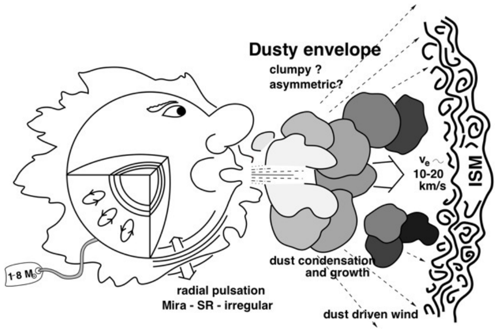

- Pulsations and dredge up
- C/O ratio → carbon stars → extreme carbon stars

Image from `www.cfa.harvard.edu`

Silicon Carbide (SiC)

- Also called carborundum or moissanite
- Found naturally in meteorites...

α-SiC vs. β-SiC

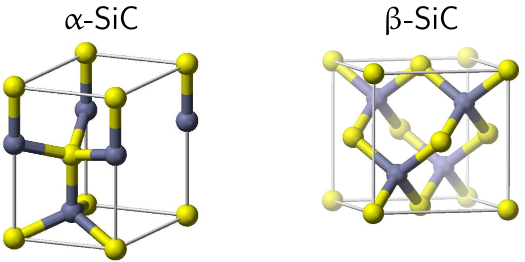

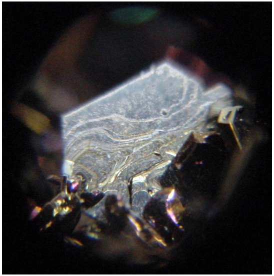

Images from Wikipedia

History of SiC Detection

- First Predicted: Fiedemann 1969 and Gilman 1969
- First Observed: Hackwell 1972
- First Sample: Bernatowicz et al. 1987
- 11 µm feature
- Low abundances but important

Presolar SiC Grains

- 99% from C-Stars (95% low mass)
- Crystalline
- 80% β-SiC
- Rarely found in cores of C grains
- Broad size distribution

Optical Parameters

Complex index of refraction

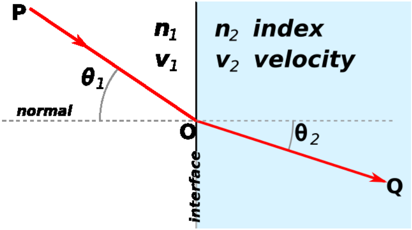

- $n + \imath k$

Birefringence

- **E**$\|$**c** (extraordinary)
- **E**$\perp$**c** (ordinary)

Images from Wikipedia

Outline

Problems with Previous SiC Data

- Mostly measure α-SiC
- Low resolution
- Used powder
- Incomplete wavelength coverage
- Models using these constants fail to match observations
- Inconsistent results from different groups

Samples

Table 2. Experimental samples: manufacturer information and references.

Polytype	Mineral Name	Grain Size	Manufacturer	Refractive Index	Comments
α-SiC	synthetic moissanite	diam. = 6.5 mm	Charles & Colvard, Ltd™	$n_o = 2.654^a$ $n_e = 2.967$	round brilliant cut gem
α-SiC	6H-SiC (gray, amber)	2 μm powder; surf. area = 9–11 m^2 g^{-1}	Alfa/Aesar (Lot # C19H06)	$n_o = 2.55$, $n_e = 2.59$ (IR) $n_o = 2.5531 + (3.34 \times 10^4) \cdot \lambda^{-2}$, $n_e = 2.5852 + (3.68 \times 10^4) \cdot \lambda^{-2b}$	hexagonal plates purity: 99.8% metals basis
α-SiC	6H-SiC (blue-gray); synthetic carborundum	several mm per crystal	unknown	$n_o = 2.654^a$ $n_e = 2.967$	Hopper crystal; (i.e., intergrown crystals)
α-SiC	6H-SiC (green, yellow)	4–8 mm wide, 0.25–1.20 Car. each	Morion Co.	$n_o = 2.654^a$ $n_e = 2.967$	green: layered, hexagonal, flat yellow: single crystal
β-SiC	3C-SiC wafer (fcc cubic)	diam = 5 μm	Rohm & Haas, Advanced Materials (Grade SC-001)	$n_{o,e} = 2.55^b$ $n_{o,e} = 2.55378 + (3.417 \times 10^4) \cdot \lambda^{-2\ c}$	CVD wafer purity: $\geq$99.9995%
β-SiC	3C-SiC gray (fcc cubic)	diam. ~2.5–25 μm	Superior Graphite	$n_{o,e} = 2.55^b$ $n_{o,e} = 2.55378 + (3.417 \times 10^4) \cdot \lambda^{-2\ c}$	equant (spherical) chips

[a] Indices of refraction for the O-ray (n_o) and E-ray (n_e) given for white light (Gaines et al. 1997) or IR λ (Goldberg et al. 2001).
[b] Values for visible light (467 nm < λ < 691 nm at T = 300 K; Schaffer & Naum 1969; Schaffer 1971). Formulae assume λ in nanometers.

Reflectance Spectra

- SiC is very hard $\Rightarrow$ hard to smooth $\Rightarrow$ back reflections
- Sanity check (assume $k \rightarrow 0$):

$$R_\nu = \frac{(n_\nu - 1)^2}{(n_\nu + 1)^2}$$

Reflectance Spectra

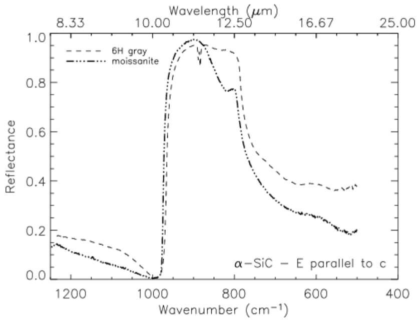

Mid- and mid+far-IR laboratory specular reflectance as a function of wavenumber (wavelength) for **E**||**c** faces of α-SiC: moissanite (dash-dot line) and gray 6H (dashed line). Laboratory values scaled to 95% maximum reflectance from 35% (moissanite) and 45% (gray 6H).

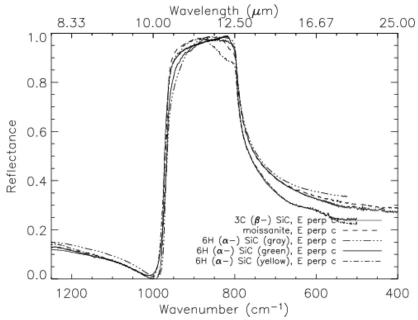

Mid- and mid+far-IR laboratory specular reflectance for **E**⊥**c** faces of β-SiC (thick solid line) and four α-SiC samples (as labeled). A mode occurs at ∼965 cm-1; polish effects account for the differences in shape of the main peak. Values scaled from 72% (β-SiC), 95% (moissanite), 84% (gray 6H), 76% (green 6H) and 84% (yellow 6H) to 98% maximum reflectance.

Classical Dispersion Analysis

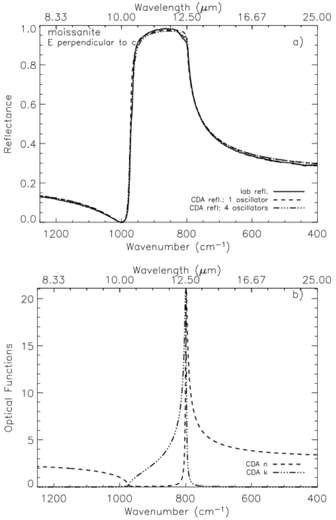

Reflectivity at near-normal incidence of moissanite (α-SiC, $\mathbf{E}\perp\mathbf{c}$ orientation) and derived n and k. a) Laboratory reflectivity spectrum (solid line, scaled to 97% maximum reflectance), calculated reflectivity fitted by 1 oscillator ($\nu = 799.0$ cm^{-1}, $FWHM = 4.0$ cm^{-1}, $f = 3.4$) (dashed line), and by 4 oscillators ($\nu_1 = 797.5$ cm^{-1}, $FWHM_1 = 1.75$ cm^{-1}, $f_1 = 2.04$; $\nu_2 = 799.0$ cm^{-1}, $FWHM_2 = 7.0$ cm^{-1}, $f_2 = 1.10$; $\nu_3 = 808.0$ cm^{-1}, $FWHM_3 = 14.0$ cm^{-1}, $f_3 = 0.28$; $\nu_4 = 970.0$ cm^{-1}, $FWHM_4 = 12.5$ cm^{-1}, $f_4 = 0.0010$) (dot-dashed line). b) n (dashed line) and k (dot-dashed line) for the 1 oscillator fit.

Classical Dispersion Analysis

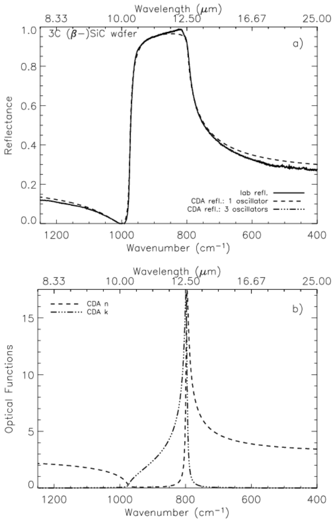

Reflectivity at near-normal incidence of β-SiC and derived *n*, *k*. a) Laboratory reflectivity spectrum (solid line, scaled to 98% maximum reflectance), calculated reflectivity for 1 oscillator (dashed line: $\nu = 797.5$ cm^{-1}, $FWHM = 6.0$ cm^{-1}, $f = 3.5$) and 3 oscillators (dot-dashed line: $\nu_1 = 797.5$ cm^{-1}, $FWHM_1 = 2.66$ cm^{-1}, $f_1 = 2.7$, $\nu_2 = 802$ cm^{-1}, $FWHM_2 = 7.0$ cm^{-1}, $f_2 = 0.68$, $\nu_3 = 875$ cm^{-1}, $FWHM_3 = 7.0$ cm^{-1}, $f_3 = 0.03$). An LO mode occurs at $\nu = 975$ cm^{-1}. b) *n* (dashed line) and *k* (dot-dashed line) for the 1 oscillator fit.

Classical Dispersion Analysis

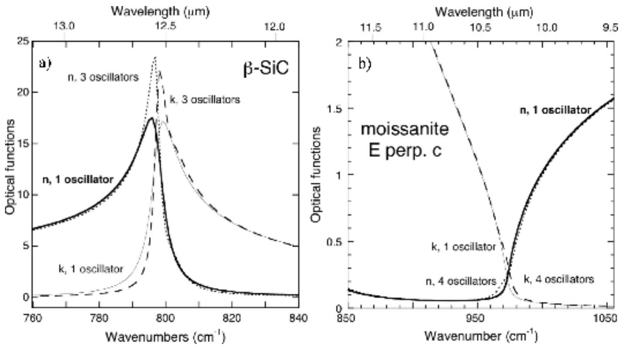

Comparison of n and k values calculated via classical dispersion for single and multiple oscillator fits: a) β-SiC (Fig. 7, Sect. 4.2), and b) α-SiC (moissanite $\mathbf{E}\perp\mathbf{c}$, Fig. 6). In a), peak heights for n and k increase if more oscillators are used in the fit. In b), adding oscillators to account for structure at $\nu \sim 800$, 970 cm^{-1} improves the fit to the laboratory reflectance spectrum, but the difference to n and k is small.

Calculated Absorbance

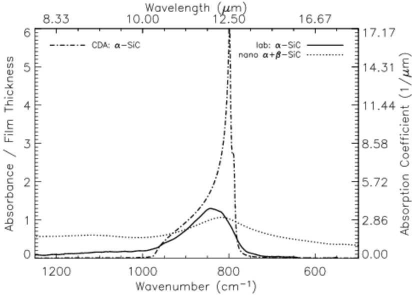

Laboratory thin film absorbances (Speck et al. 1999; Speck et al. 2005) divided by estimated sample thicknesses ($d \sim 0.5$ μm) compared to calculated classical dispersion analysis absorbance coefficients for α-SiC. Calculated absorbance coefficients for the remaining α-SiC samples are indistinguishable.

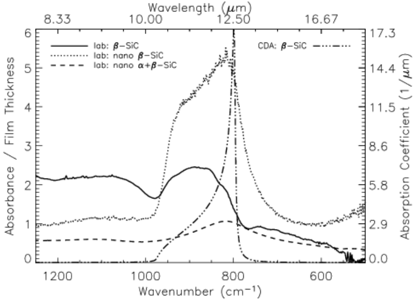

Laboratory thin film absorbances (Speck et al. 1999, 2005) divided by estimated sample thicknesses ($d \sim 0.15$μm for β-SiC, 0.5 μm for nano samples) compared to calculated classical dispersion analysis absorbance coefficients for a 1 oscillator fit to β-SiC (Fig. 7). Given the uncertainty in estimated sample thicknesses, laboratory values can be scaled by factors of 3–5.

Outline

Previous Models

Table 1
Previous Models of Extreme Carbon Stars with 11 μm Absorption Features

Star	Composition[a] (SiC%)	Grain-Size (μm)	$\tau_{11.3\,\mu m}$	Drop-off	R_{in}[b] ($\times 10^{-4}$ pc)	T_{in} (K)	$\dot{M}$[b] ($M_\odot$ yr^{-1})	References
00210+6221	0	0.1	4.5	3.00	0.362/D	1000	$12 \times 10^{-5}/D$	2
01144+6658	8	0.1	4.84			1000	9.50×10^{-7}	4
06582−1507	0	...	5.15			1000	1.08×10^{-4}	1
	0	0.1	2.1	2.25	1.23	1000	2.59×10^{-4}	2
17534−3030	0	0.1	4.4	2.50	1.39	1000	8.20×10^{-4}	2
19548+3035	0	0.1	2.5	2.50	1.17	1000	3.89×10^{-4}	2
21318+5631	0	...	1.36			700	1.10×10^{-4}	3
23166+1655	0	0.1	1.12			650	5.50×10^{-7}	4
	30	...	7.85			1000	3.30×10^{-5}	1
	0	...	1.19			650	1.00×10^{-4}	3

Notes. Neither Volk et al. (1992) nor Groenewegen (1995) specify the grains sizes used in their models.
[a] Composition assumes remainder dust is carbon. In all but Volk et al. (1992) the carbon is amorphous; Volk et al. (1992) uses graphitic carbon.
[b] Originally quoted as a function of distance. Value quoted here assume distances from Groenewegen et al. (2002), listed in Table 5.
References. (1) Volk et al. (1992); (2) Volk et al. (2000); (3) Groenewegen (1995); (4) Groenewegen et al. (1998).

Observations

- 10 Sources
- ISO SWS

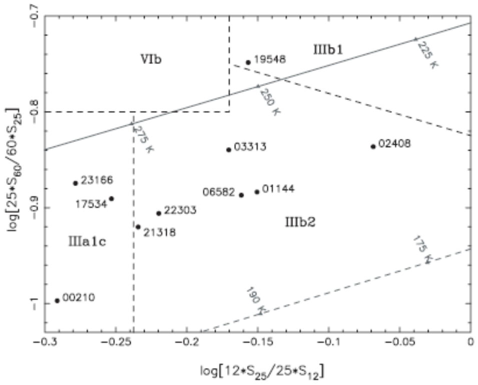

Regions in the IRAS colorcolor diagram populated by extreme carbon stars (see the text for details). The blackbody curve is indicated by the solid gray line. The modified blackbody $[B(T,\lambda) \times \lambda^{-1}]$ is indicated by the dashed gray line.

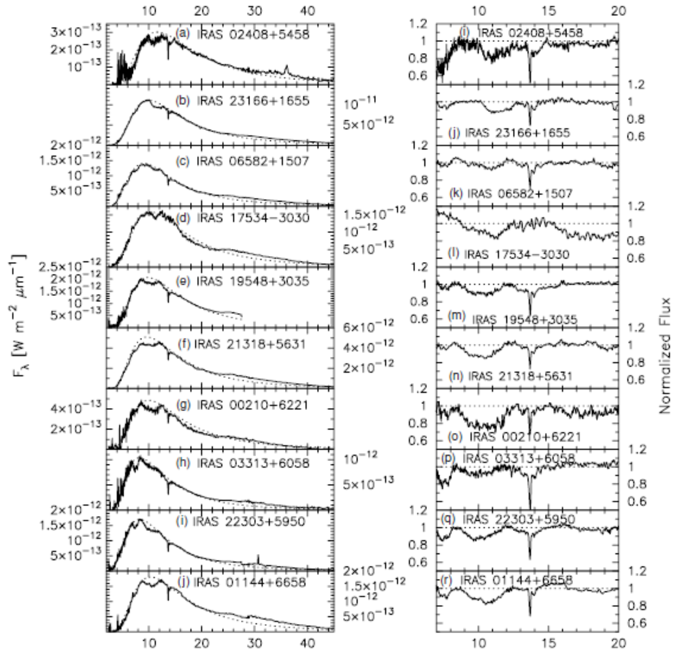
(a) IRAS 02408+5458
(b) IRAS 23166+1655
(c) IRAS 06582+1507
(d) IRAS 17534−3030
(e) IRAS 19548+3035
(f) IRAS 21318+5631
(g) IRAS 00210+6221
(h) IRAS 03313+6058
(i) IRAS 22303+5950
(j) IRAS 01144+6658
(i) IRAS 02408+5458
(j) IRAS 23166+1655
(k) IRAS 06582+1507
(l) IRAS 17534−3030
(m) IRAS 19548+3035
(n) IRAS 21318+5631
(o) IRAS 00210+6221
(p) IRAS 03313+6058
(q) IRAS 22303+5950
(r) IRAS 01144+6658
F$_\lambda$ [W m^{-2} μm^{-1}]
Normalized Flux

Observations

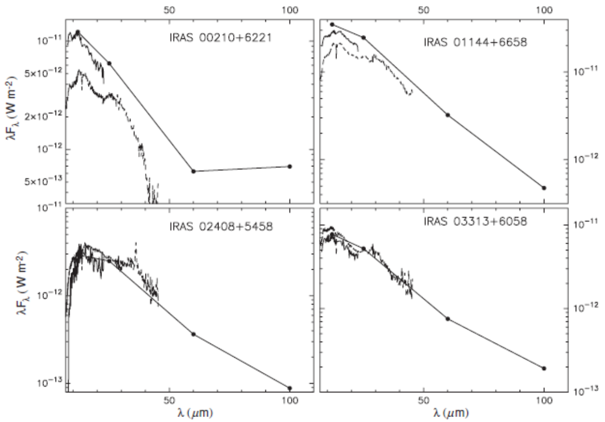

ISO SWS spectra of sample extreme C-stars together with IRAS 12, 25, 60, and 100 μm photometry points and IRAS LRS spectra. Solid line = IRAS spectrum; points: IRAS photometry points; dashed line: ISO SWS spectrum. The *y*-axis is the flux (λF_λ) in W m^2; the *x*-axis is the wavelength in μm.

Grain Size

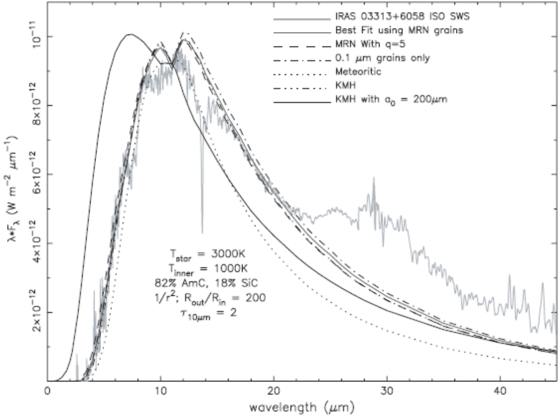

Effect of grain-size distributions on the model SED. In all cases, the model parameters are identical except for the grain-size distribution. See Section 3.2 for detailed description of the grain-size distributions. The gray line shows the ISO-SWS spectrum of IRAS 03313+6058 for comparison.

Dust Condensation

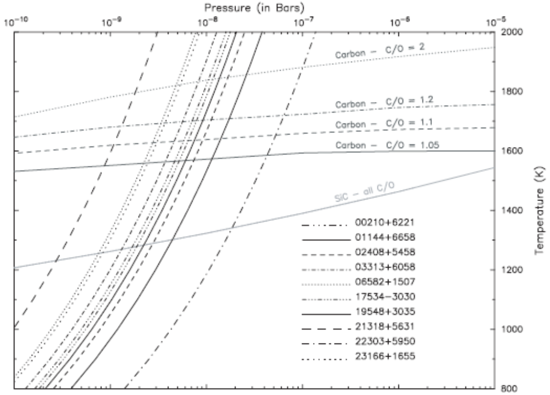

Pressure-temperature space for the dust condensation region around extreme carbon stars (assumes solar metallicity). The gray lines indicate the condensation temperature for a given pressure as calculated by Lodders & Fegley (1995). The black lines indicate the P-T paths for the outflowing gas from our sample stars; (top) as calculated from the published CO mass-loss rates and expansion velocities (see Section 3.4.2 for details); and (bottom) as calculated from the modeled dust temperature radial profile.

Best Fits

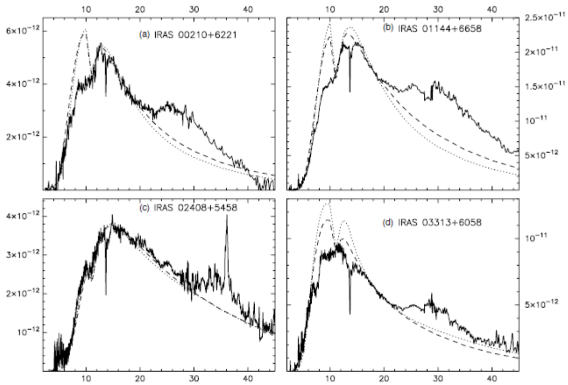

Best-fit models (part 1). Solid line: ISO-SWS spectrum; dashed line: best-fit model using MRN grain-size distribution; dotted line: best-fit model using "meteoritic" grain-size distribution; the x-axis is the wavelength (μm); the y-axis is the flux (λF_λ) in W m^2. In all cases, $T = 3000$ K and $T_{\rm inner} = 1800$ K. Model parameters are listed in Table 4.

Best Fits

Table 4
Model and Derived Parameters

IRAS Number	T_*	T_{inner}	R_{out}/R_{in}	$\tau_{10\,\mu m}$	Composition SiC%	Composition Graphite %
			MRN Grain-Size Distribution			
00210+6221	3000	1800	10	6	10	90
01144+6658	3000	1800	15	6.5	10	90
02408+5458	3000	1800	20	12	3	97
03313+6058	3000	1800	15	4	10	90
06582+1507	3000	1800	10	6	5	95
17534−3030	3000	1800				
19548+3035	3000	1800	15	6.5	5	95
21318+5631	3000	1800	10	8	3	97
22303+5950	3000	1800	15	4	10	90
23166+1655	3000	1800	15	7.5	3	97
			Meteoritic Grain-Size distribution			
00210+6221	3000	1800	10	6	30	70
01144+6658	3000	1800	10	7.5	30	70
02408+5458	3000	1800	100	8.5	12	88
03313+6058	3000	1800	500	3.25	40	60
06582+1507	3000	1800	10	6	20	80
17534−3030	3000	1800	20	5	35	65
19548+3035	3000	1800	100[a]	4.75	25	75
21318+5631	3000	1800	100	5	20	80
22303+5950	3000	1800	500	3.25	40	60
23166+1655	3000	1800	50	5	25	75

Note. [a] Models with $R_{out}/R_{in} > 100$ can be accommodated because the data beyond 26 μm is poor and ignored, but based on the similarity of this source to IRAS 21318+5631, we assume this is a good upper limit.

Dust Shell Ages

Table 6
Size and Age of the Dust Shells

IRAS	MRN Size Distribution			Meteoritic size distribution		
Number	R_{in} (10^{14} cm)	R_{out} (10^{14} cm)	Age (yrs)	R_{in} (10^{14} cm)	R_{out} (10^{14} cm)	Age (yr)
00210	2.68	26.8	50.9	2.78	2.78	52.8
01144	2.74	41.1	72.4	3.08	30.8	54.2
02408	4.11	82.2	236.8	2.99	299	861.3
03313	2.17	32.6	74.2	2.10	1050	2393.7
06582	2.73	27.3	63.1	2.72	27.2	62.9
17534	2.51	50.2	83.7	2.51	50.2	83.7
19548	2.78	41.7	59.3	2.38	238	338.2
21318	3.18	31.8	51.4	2.41	241	389.6
22303	2.24	33.6	58.2	2.10	1050	1818.2
23166	2.88	43.2	90.7	2.45	123	257.1

Notes. Calculation of R_{out} is based on the model parameters listed in Table 4. R_{in} comes from the model output. The calculation of the age of the dust shells is then done using these data and the observed expansion velocities listed in Table 5.

Summary

- SiC forms in C-Stars
- Provides major IR feature
- ISM grain sizes a good fit (small grains)
- Dust shells must have very short lifetimes
- So-so model fit $\Rightarrow$ O-chemistry?

References

- Speck, A. K. 1998, Ph.D. Thesis
- Pitman, K. M., Hofmeister, A. M., Corman, A. B., & Speck, A. K. 2008, A&A, 483, 661
- Speck, A. K., Corman, A. B., Wakeman, K., Wheeler, C. H., & Thompson, G. 2009, ApJ, 691, 1202